IEEE Access
Multidisciplinary | Rapid Review | Open Access Journal

Received July 14, 2019, accepted July 19, 2019, date of publication July 24, 2019, date of current version August 9, 2019.

Digital Object Identifier 10.1109/ACCESS.2019.2930907

Resiliency of Distribution Systems Incorporating Asynchronous Information for System Restoration

JUAN C. BEDOYA[1], JING XIE[2], YUBO WANG[3], XI ZHANG[3], AND CHEN-CHING LIU[1], (Fellow, IEEE)

[1]Power and Energy Center, The Bradley Department of Electrical and Computer Engineering, Virginia Tech, Blacksburg, VA 24061, USA
[2]Pacific Northwest National Laboratory, Seattle Research Center, Seattle, WA 98109, USA
[3]Siemens Corporate Technology, Princeton, NJ 08540, USA

Corresponding author: Juan C. Bedoya (bedojuan@vt.edu)

This work was supported in part by the SIEMENS Corporate Technology, in part by the Dominion Energy, and in part by the U.S. Department of Energy (DOE) through the Virginia Tech agreement under Grant AT-45607 of 2018.

ABSTRACT Resiliency of distribution systems under extreme operating conditions is critical, especially when the utility is not available. With the large-scale deployment of distributed resources, it becomes possible to restore critical loads with local non-utility resources. Distribution system operators (DSOs) need to determine the critical loads to be restored, considering limited resources and distribution facilities. Several studies on resiliency have been conducted for the restoration of distribution systems. However, the inherent asynchronous characteristic of the information availability has not been incorporated. With incomplete and asynchronous information, decisions may be made that result in underutilization of generation resources. In this paper, a new distribution system restoration approach is proposed, considering uncertain devices and associated asynchronous information. It uses a two-module architecture that efficiently optimizes restoration actions using a binary linear programming model and evaluates their feasibility with unbalanced optimal power flow. Networked microgrids are included in the model. The IEEE 123-node test feeder is used for validation. The results show that asynchronous messages may affect the restoration actions significantly and the impacts can be mitigated by the proposed decision support tool for the DSOs.

INDEX TERMS Binary linear programming, decision making with asynchronous information, distribution systems resiliency, three-phase unbalanced optimal power flow.

I. INTRODUCTION

For decades, the electric energy distribution systems have been designed to serve the load while maintaining a high-level reliability based on various indices [1]. However, it is becoming evident that power grid's capabilities to respond and adapt under extreme conditions such as catastrophic outages are critical to achieve resiliency [2]. Resiliency is a multidisciplinary concept that has attracted much attention from government and industry. For instance, in 2013, The US White House Office of Press published presidential policy directive PPD-21, in which resiliency for critical infrastructure was defined as the systems' adaptation to continuous changing conditions, system disruptions, and recovery from deliberate attacks, accidents, incidents, and threats [3]. Resiliency is a national priority due to the high socioeconomic impact of large and extended power outages [4]. Indicators include the estimated $26 billion dollars annual costs of 5-minutes (or longer) power outages in the U.S. [5], extensive losses due to natural disasters, and massive power outages (Hurricanes Florence and Michael in 2018, Midwestern floods in 2008, among others [6]–[11]). There are also considerations of increasing global warming [12]. The power infrastructure is one of the most critical services for the society; therefore, in this research the enhancement of resiliency is incorporated in the formulation of distribution system restoration problem following catastrophic outages.

Distribution system restoration is a multidisciplinary subject involving *real-time* optimization and *asynchronous* communication for *decision-making*. Military and civilian systems deal with similar problems, such as the spanning tree approach in the traveling-salesman problem, power system resource coordination, embedded processing system, offshore wind turbine maintenance scheduling, and switching control [13]–[18]. In distribution systems, the goal is to determine the needed actions to serve critical loads using the

The associate editor coordinating the review of this manuscript and approving it for publication was Baoping Cai.

available infrastructure, resources, and communication [2]. Much research based on topology reconfiguration has been conducted for the restoration problem. The main assumption in the reconfiguration task is that faulted grid sections can be isolated, and loads can be picked up using an alternative path from a backup feeder. Solutions based on multiagent models, artificial intelligence, Lagrange relaxation optimization, and heuristic techniques have been reported [19]–[23]. However, these methods rely on power from the substation to serve the feeders, making them potentially infeasible when the utility system is not available due to the extreme events. During major disasters, the availability of transmission and distribution facilities for delivery of power is limited.

With the increasing penetration of renewable generation resources, proactive loads, smart meters, remote-controlled switches, intelligent devices, and energy storage, some applications have been proposed to improve the reliability and resiliency of the grid [24]–[27]. Researchers proposed an approach based on mix-integer linear programming to determine islanded microgrids that optimally supply critical loads after severe power outages [28], [29]. A mixed integer non-linear optimization approach to maximize critical load restoration, using constant current load models is proposed in [30]. A sequential service restoration approach for distribution system restoration based on mixed integer programming and a linearized model power flow model is proposed in [31]. A microgrid approach to system restoration using spanning tree search is proposed in [32]. A decentralized multiagent approach using DG islanding is proposed in [33]. An agent-based approach to reliability optimization in the restoration process, considering load balancing as a constraint, is presented in [34]. A decentralized control architecture to improve resiliency is developed [35]. DGs for service restoration considering technical constraints for inrush currents, DGs synchronization, frequency limits, among others, are studied [36], [37]. Interconnected microgrids for resilience improvement are also proposed [38], [39]. A multi-stage restoration strategy that considers the outage duration uncertainty through a maximum likehood estimation approach is presented in [40].

Current restoration approaches assume that information regarding the status of the distribution system is known. In reality, partial knowledge of the available infrastructure, uncertainty of the status of available assets, and communication capabilities, make the restoration problem a *real-time* and *asynchronous decision-making* problem. The information is presented to the distribution system operator (DSO), or whoever performs the restoration role, in irregular time rates, i.e., asynchronously. Neglecting the asynchronous nature of information may lead to scenarios where available resources are underutilized, reducing the capability to serve critical load.

In this paper a new two-module approach for distribution system restoration is proposed to incorporate sources of uncertainty and asynchronous information. The first module maximizes a resiliency function based on binary linear programming (BLP). In contrast with traditional approaches,

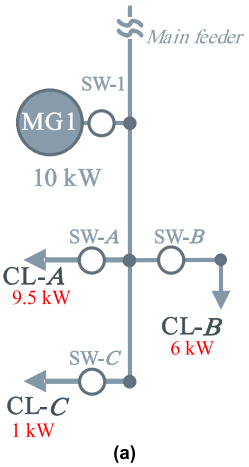

Mssg-A1: SW-A is operable.
Mssg-B1: SW-B is operable.
Mssg-C1: SW-C is operable.
Mssg-A2: SW-A is NOT operable.
Mssg-B2: SW-B is NOT operable.
Mssg-C2: SW-C is NOT operable.
(b)

Inst-A: Instruction given to close SW-A
Inst-B: Instruction given to close SW-B
Inst-C: Instruction given to close SW-C
Conf-A: Confirmation that SW-A was successfully closed.
Conf-B: Confirmation that SW-B was successfully closed.
Conf-C: Confirmation that SW-C was successfully closed.
(c)

FIGURE 1. Distribution system, messages and instructions during the restoration process. (a) Topology of the system. (b) Potential messages to be send by field crew to DSO. (c) Potential instructions to be given by DSO to field crew.

critical loads are supplied by microgrids in an islanded mode. Networked microgrids result in an improved restoration capability and better utilization of available resources. The result of Module-I is a sequence of switching actions, to be executed during the restoration stage, so that networked microgrids can supply critical loads in the system. Module-II evaluates the proposed restoration plan by solving a three-phase unbalanced optimal power flow (3Ph-OPF). Steady state conditions are evaluated and integer decision variables for reactive power compensation are considered, using the second-order conic relaxation of the optimal power flow for distribution systems [41]–[43]. Also, a smart algorithm for the detection of islanded areas and an area independent 3Ph-OPF formulation have been implemented. The contributions of this paper are:

- Incorporating asynchronous information in decision-making of distribution system restoration.
- Optimal matching of networked microgrids with critical loads.
- Two-module architecture enabling the evaluation of restoration actions and its feasibility by unbalanced 3Ph-OPF.
- Identification of islanded areas based on the proposed system restoration topology.
- Formulation of 3Ph-OPF for any number of islanded areas in the system.

To the best of the authors' knowledge, the effect of asynchronous and uncertain information in distribution system restoration has not been reported. Remaining sections of this paper present the effect of asynchronous messages in the resiliency problem and the two-module architecture. Finally, the proposed method is validated with the IEEE 123-node test feeder.

II. MOTIVATION

The asynchronous characteristic in the restoration problem is introduced using a simple distribution system in Figure 1.

Assume that the utility has become unavailable and only a 10 kW DG (or a microgrid) is available to serve the three critical loads (CL-A, CL-B, and CL-C) with rated powers 9.5 kW, 6 kW, and 1kW, respectively. The goal is to serve as much critical load as possible assuming that CL-B is two times more critical than CL-A, and CL-A is as critical as CL-C. The distribution system has switches SW-1, SW-A, SW-B, SW-C, to connect or isolate DG and loads from the main feeder. Assuming that all switches are open, DSO knows that SW-1 is operable, but it is uncertain whether SW-A, SW-B, and SW-C, are operable or not, say, due to damage. Hence, DSO sends the field crew to check the status of switches SW-A, SW-B, and SW-C. As a result, the system operator expects to receive three messages. These messages will be received *asynchronously*. The possible messages and DSO operation instructions are presented in Figure 1.

The optimal restoration actions, denoted as ''original restoration plan'' (if all switches are operable), are ''Inst-B'' and ''Inst-C.'' In this case 6 kW (CL-B) and 1 kW (CL-C) are restored, considering the level of criticality. Note that if SW-B is not operable, the ''back-up restoration plan'' is simply pick up CL-A. One potential approach is ''waiting'' until all information is available (synchronous mode). This may not be a proper DSO decision given the urgency to serve the critical loads. Another approach is that DSO makes decisions as it receives information from the field crew or remote monitoring toward the original restoration plan. It is usual in power system restoration to not interrupt service once a critical load is restored. Then, potential scenarios of set messages, instructions, and confirmations are:

1) ''Mssg-A1'' – ''Mssg-B2'' – ''Inst A'' – ''Conf-A, or 2) ''Mssg-C1'' – ''Inst-C'' – ''Conf-C'' – ''Mssg-B2''.

Note that in the first scenario, DSO intends to implement the ''original restoration plan;'' however, as soon as DSO becomes aware of the ''not operable'' status for SW-B (having received operability message for SW-A), proceeds with the ''back-up restoration plan'' to serve CL-A. In the second scenario, as soon as operability of SW-C is received, DSO proceeds with instructions of the ''original plan'' by closing switch SW-C (Inst-C), and later receives a confirmation of the action. Unfortunately, after the first restoration action is performed, the non-operability message of SW-B is received; the DSO cannot execute the ''back-up plan'' anymore, given that CL-C has already been restored. Moreover, CL-A cannot be restored along with CL-C given the resources capacity limitations. In this scenario, because of inappropriate management of asynchronous messages, available resources (10 kW) are underutilized (only 1 kW of critical load is restored).

III. PROPOSED ARCHITECTURE AND ASYNCHRONOUS INFORMATION

A. ARCHITECTURE

The proposed distribution system restoration approach is based on a sequential two-module structure. The first module (Module-I) determines the required set of actions to link generation resources (PVs, energy storage devices, microgrids, etc.) with critical loads in the system. After a major event, the restoration plan provided by Module-I considers the effect of asynchronous messages received by the DSO once the field crew evaluates the ''uncertain'' operability of the available infrastructure. The plan provided by Module-I is a list of switching actions that DSO can execute either simultaneously or sequentially, depending on the available facilities. Before execution of the restoration plan provided by Module-I, Module-II evaluates if there is any power system security concern or risk by configurations generated by Module-I. The security check is based on a 3Ph-OPF. The restoration actions are executed if the constraints of the OPF security problem are satisfied. Moreover, if necessary, Module-II evaluates mitigation actions, in case of security issues, based on reactive power compensation. Available capacitor banks are connected to the system and transformer tap changers are used to improve voltage profiles. If mitigation actions are not able to resolve the security issues, a new restoration plan is determined by Module-I by considering alternate paths along which restrictive operational conditions can be avoided.

The two-module structure proposed in this work presents a novel mechanism to assign available power supply to the most critical load (Module-I) and take into account power system security operability (Module-II). The assignment of resources is achieved through a binary linear programming optimization model, while the system security is pursued through the minimization of system voltage violations (minimizing nodal reactive power injection using a 3Ph-OPF). Each module has its own computational challenges. For instance, Module-I is characterized by a large number of binary variables that indicate the paths, islanded areas, and switching-sequential energization actions to meet resources and critical loads. Challenges of Module-II come from non-linear relations between bus voltages, branch current, branch power flows, three phase system imbalance, and phase couplings. The two-module structure is proposed instead of a unified approach due to the computationally requirements and scalability aspects of the algorithm. For instance, a typical small distribution network will have hundreds of nodes. The restoration problem as a unified algorithm for resource assignment and security would result in a non-linear integer optimization problem. Finding a feasible solution in the restoration plan can be a cumbersome task for which its optimality cannot be validated. Additionally, characteristics of a joint solution in an optimization model would result in a combinatorial problem that requires a prohibitive computational time.

B. MANAGEMENT OF ASYNCHRONOUS INFORMATION

Diverse resiliency metrics and functions have been proposed for engineering systems. In [44], a logarithmic based resiliency function is proposed. A resiliency metric based on the system capacity at different states is presented in [45]. In [46], a resiliency metric based on distribution system performance after a major power outage is proposed. As shown

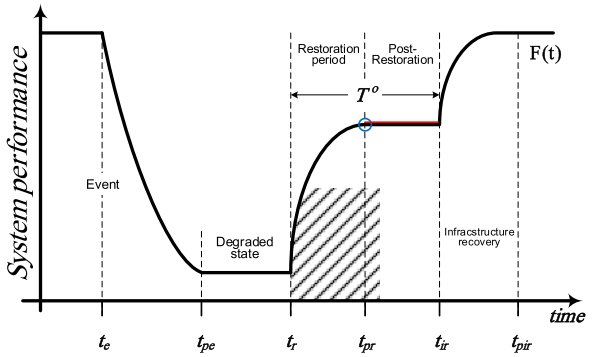

FIGURE 2. System performance function. A conceptual resiliency function associated with an extreme event [46].

in Figure 2, performance of the system varies at each different state of the distribution system due to a major event and restoration actions. The system performance function $F(t)$, as defined in [46], is the total power supplied to critical loads weighted by their priority (critical factor) and the resiliency metric is defined as the area under $F(t)$ between the initial execution of the restoration actions (t_r) and the time for system recovery (t_{ir}). If the system status, available devices, and available infrastructure is known, DSO can estimate the time required to restore system's critical infrastructure (time interval T^O) [2].

In this work, the management of the asynchronous information arrival and decision making are based on a "waiting time" signal calculated by the DSO. This waiting time is calculated based on an "ideal scenario" and an "actual scenario." The "ideal scenario" refers to the scenario where comprehensive information can be retrieved. In this scenario, after the power outage has occurred, the system status, available devices, and available infrastructure are known by the DSO without the need to send field crew to retrieve the above information. In this case, DSO can estimate the required time to restore system's critical infrastructure (time interval T^O) based on expert knowledge and previous experience [2]. On the other hand, the "actual scenario" refers to the state where limited information can be retrieved. This state considers the limited information that is immediately available after the major power outage. In this case, it is expected that a lower level of critical load is restored.

In the "ideal" scenario (i.e. required information is known) the DSO is able to determine the optimal amount of critical load that can be restored by using the two-module based restoration approach (described in Section III-A. Details in Section IV and Section V). Hence, this amount of critical load to be "ideally" restored represents an upper bound (UB) for the performance of the system in time interval T^O. Similarly, for the actual scenario, DSO is also able to determine the amount of load that can be restored. This amount defines a lower bound (LB) of the critical load that can be restored.

After a critical event (i.e. major power outage), DSO may know the status of some assets but not the operability status of other facilities required to execute the optimal restoration plan. For instance, if the system has some non-remote-controlled switches, for which DSO does not know their operability, the DSO can decide to send the available field crew to verify if it is possible to operate the switches involved in the restoration plan. Each switch operability status represents a source of ***uncertainty***, while information sent by the field crew to DSO constitutes multiple ***asynchronous*** messages. Therefore, the DSO faces the predicament of *how long DSO should wait for the asynchronous information to arrive before executing further restoration actions*. An extended waiting time can lead to conditions where resources are underutilized, and critical load is not restored in a timely manner.

A maximum waiting time t_w, before DSO proceeds with an alternative restoration plan, can be calculated considering:

1) The amount of load restored and duration of the restored period, if DSO decides not to wait for messages from the field crew and proceed with restoration actions based on the available information. In this case, LB amount of load would be restored during the entire time interval T^O.
2) If DSO decides to wait for messages from the field crew, DSO will be able to restore UB units of load during the period $T^O - t_w$.

Therefore, the waiting decision is based on whether the results given in the second scenario are better than results given in the first one. Thus, waiting time t_w is determined by

$$UB \cdot \left(T^O - t_w\right) \geq LB \cdot T^O \tag{1}$$

$$t_w \leq \frac{(UB - LB) \cdot T^O}{UB} \tag{2}$$

For the second scenario of asynchronous messages in Section II, once DSO receives message "Mssg-C1," a waiting time t_w should be established before proceeding with instruction "Inst-C." DSO knows that the best scenario for restoration is to supply 9.5 kW of critical load. Also, DSO knows that the worst scenario is to supply only 1 kW of critical load. Hence, applying the criteria in (1) and IV, DSO determines that $t_w = 89.4\% \cdot T^O$ is the appropriate waiting time before proceeding to pick up load C.

The proposed approach can be extended to include further scenarios such as those with different power supply levels arising from variable renewable energy resources. For instance, power production from a solar panel array can be considered through three different scenarios (high, medium, and low) of energy supply. This information can be considered in the calculation of parameters UB and LB and the minimum waiting time can be selected accordingly. The renewable production uncertainty can become a hurdle for the assumption that once a critical load has been energized, its power supply should not be interrupted. To avoid those scenarios, variable renewable resources should be complemented with energy storage devices.

IV. MODULE-I

Module-I solves a BLP model that determines the set of switches to be closed and lines to be energized at each time step to maximize the amount of restored critical loads. The optimization model is described here.

A. SETS

S_M :	Set of available microgrids
S_S :	Set of switches
S_{PH} :	Set of phases, $S_{PH} = \{a, b, c\}$
S_L :	Set of lines
S_B :	Set of buses
S_{B-N-M} :	Set of buses without microgrids
S_{B-W-M} :	Set of buses with microgrids
S_{CL} :	Set of critical loads
S_T :	Set of time, $S_T = \{T_0, T_0+T_{\text{interval}}, \ldots, T\}$
S_{RT} :	Set of run time, $S_{RT} = \{T_0 + T_{\text{interval}}, T_0 + 2T_{\text{interval}}, \ldots, T\}$
$S_L^{\text{Bus}i}$:	Set of lines connected with bus i
$S_S^{\text{Bus}i}$:	Set of switches connected with bus i

B. SYSTEM PARAMETERS

$I_{B1}^{\text{line}i}, I_{B2}^{\text{line}i}$:	Indices of the two buses connected to line i
$I_{B1}^{\text{sw}i}, I_{B2}^{\text{sw}i}$:	Indices of the two buses connected to switch i
$I_B^{\text{M}i}$:	Index of the bus connected with microgrid i
$I_B^{\text{CL}i}$:	Index of the bus connected with critical load i
$P_{\text{M}i}$:	Available real power of microgrid i
$P_{\text{CL}i}^{\text{PH}j}$:	Real power of critical load i at phase j
$W_{\text{CL}i}^{\text{PH}j}$:	Critical level of critical load i at phase j
T_0 :	Starting time
T :	Ending time
T_{interval} :	Time interval
T_S^i :	Minimum elapsed time of operating switch i
T_L^i :	Minimum elapsed time of energizing line i
$\beta = 0.85$:	Percentage of capacity needed to pick up critical load within each island

C. DECISION VARIABLES

The decision variables of the BLP model to be solved in Module-I, are presented next.

$u_S(i,t)$: *(Binary)*	1 if switch i is closed at time t, 0 if otherwise. $i \in S_S$, $t \in S_T$
$u_L(i,t)$: *(Binary)*	1 if line i is energized at time t, 0 if otherwise. $i \in S_L$, $t \in S_T$
$u_{CL}(i,t,k)$: *(Binary)*	1 if critical load i is energized and has a path connected to microgrid k, 0 if otherwise. $i \in S_{CL}$, $t \in S_T$, $k \in S_M$
$u_{CL}(i,t)$: *(Auxiliary and Binary)*	1 if $\sum_{k \in S_M} u_{CL}(i,t,k) \geq 1$ at time t, 0 if otherwise. $i \in S_{CL}$
$u_B(i,t,k)$: *(Binary)*	1 if bus i is energized at time t and has a path connected to microgrid k, 0 if otherwise. $i \in S_B$, $t \in S_T$, $k \in S_M$
$u_M(i,t,k)$: *(Binary)*	1 if microgrid i is energized at time t and has a path connected to microgrid k, 0 if otherwise. $i \in S_M$, $t \in S_T$, $k \in S_M$

D. OBJECTIVE FUNCTION

The objective function of the BLP problem is to maximize the critical load to be restored at the end of the restoration and post restoration period [46] along with minimization of the number of required switching actions. In this case, the rated power of the critical load is quantified along with its priority level.

$$\underset{\text{Decision variables}}{\text{Max}}\ \pi = a_1 \left(\sum_{i \in S_{CL}} \sum_{j \in S_{PH}} P_{CLi}^{PHj} \cdot W_{CLi}^{PHj} \cdot u_{CL}(i,T) \right) + a_2 \left(\sum_{i \in S_S} \sum_{t=0}^{T} u_s(i,t) \right) \quad (3)$$

Coefficients $a_1 > 0$ and $a_2 < 0$, are used to combine individual objectives, maximization of restored load and minimization of the number of switching actions, respectively. Magnitudes of these coefficients may be tuned up according to the relevance that DSO desires to provide to each of the individual objectives. In the proposed work the main goal is to supply restore the largest amount of critical load. Finally, the product $P_{CLi}^{PHj} \cdot W_{CLi}^{PHj}$ considers not only the critical load rated power but also its critical level. For instance, consider two critical loads CL-X and CL-Y with rated power 5 kW - 7 kW, and criticality factors 3 - 2, respectively. Although CL-Y rated power is greater than CL-X, the objective function will prioritize CL-X over CL-Y given that the product 5×3 is larger than 7×2.

E. CONSTRAINTS

1) INITIAL CONDITIONS

The constraints for lines and switches in the ILP model are very similar. These constraints with the initial conditions are listed next:

All switches are open at the initial time step.

$$u_S(i, T_0) = 0, \quad \forall i \in S_S \quad (4)$$

All lines are de-energized at the initial time step.

$$u_L(i, T_0) = 0, \quad \forall i \in S_L \quad (5)$$

All critical loads are de-energized at the initial time step.

$$u_{CL}(i, T_0, k) = 0, \quad \forall i \in S_{CL} \quad (6)$$

Buses that do not have a microgrid connected are de-energized at the initial time step.

$$u_B\left(i, T_0, k\right) = 0, \quad \forall i \in \mathrm{S_{B-N-M}}, \quad k \in \mathrm{S_M} \tag{7}$$

Each bus that has a microgrid connected is energized at the initial time step, together with its connected microgrid.

$$u_B\left(I_B^{\mathrm{M}k}, T_0, k\right) = 1, \quad \forall k \in \mathrm{S_M} \tag{8}$$

$$u_B\left(I_B^{\mathrm{M}k}, T_0, l\right) = 0, \quad \forall k, l \in \mathrm{S_M}, \text{ and } l \neq k \tag{9}$$

$$u_M\left(k, T_0, k\right) = 1, \quad \forall k \in \mathrm{S_M} \tag{10}$$

$$u_M\left(k, T_0, l\right) = 0, \quad \forall k, l \in \mathrm{S_M}, \text{ and } l \neq k \tag{11}$$

2) LINE CONSTRAINTS

Line i can be energized at time t, once one of its two connected buses is energized at time $t - T_L^i$. Once a line is energized, its two connected buses are both energized at the same time step and interconnected with the same microgrid(s).

$$\begin{aligned} u_L(i,t) \leq \sum_{k \in \mathrm{S_M}} \Big\{ & u_B(I_{B1}^{\mathrm{line}i}, t - T_L^i, k) \\ & + u_B(I_{B2}^{\mathrm{line}i}, t - T_L^i, k) \Big\} \\ & \forall i \in \mathrm{S_L}, t \in \mathrm{S_{RT}} \end{aligned} \tag{12}$$

$$\begin{aligned} u_L\left(i,t\right) \leq 1 - \left(u_B\left(I_{B1}^{\mathrm{line}i}, t, k\right) - u_B\left(I_{B2}^{\mathrm{line}i}, t, k\right)\right) \\ \forall i \in \mathrm{S_L}, \quad t \in \mathrm{S_{RT}}, \quad k \in \mathrm{S_M} \end{aligned} \tag{13}$$

$$\begin{aligned} u_L\left(i,t\right) \leq 1 - \left(u_B\left(I_{B2}^{\mathrm{line}i}, t, k\right) - u_B\left(I_{B1}^{\mathrm{line}i}, t, k\right)\right) \\ \forall i \in \mathrm{S_L}, \quad t \in \mathrm{S_{RT}}, \quad k \in \mathrm{S_M} \end{aligned} \tag{14}$$

Once a line is energized, it cannot be de-energized.

$$u_L\left(i, t-1\right) \leq u_L\left(i,t\right), \quad \forall i \in S_L, \quad t \in S_{RT} \tag{15}$$

3) BUS ENERGIZING CONSTRAINTS

$$\begin{aligned} u_B\left(i,t,k\right) \leq \sum_{j \in \mathrm{S_L^{Bus}}i} u_L\left(j,t\right) + \sum_{j \in \mathrm{S_S^{Bus}}i} u_S\left(j,t\right) \\ \forall i \in \mathrm{S_{B-N-M}}, \quad t \in \mathrm{S_{RT}}, \quad k \in \mathrm{S_M} \end{aligned} \tag{16}$$

$$u_B\left(I_B^{\mathrm{M}k}, t, k\right) = 1, \quad \forall t \in \mathrm{S_{RT}}, \quad k \in \mathrm{S_M} \tag{17}$$

To pick up bus i at time t, at least one of the lines or switches connected to bus i is energized at time t. The set of buses connected with microgrids is assumed to be energized.

4) SWITCH ENERGIZING CONSTRAINTS

Switch i can be energized at time t, once one of its two connected buses is energized at least T_S^i steps before.

$$\begin{aligned} u_S(i,t,k) \leq \sum_{k \in \mathrm{S_M}} \Big\{ & u_B(I_{B1}^{\mathrm{switch}i}, t - T_S^i, k) \\ & + u_B(I_{B2}^{\mathrm{switch}i}, t - T_S^i, k) \Big\} \\ & \forall i \in \mathrm{S_S}, \quad t \in \mathrm{S_{RT}} \end{aligned} \tag{18}$$

5) CLOSED SWITCH CONSTRAINTS

At time t, once a switch i is in a closed status, its two connected buses are both energized and have a path connected to the same microgrid(s).

$$\begin{aligned} u_S\left(i,t\right) \leq 1 - \Big(u_B\Big(I_{B1}^{\mathrm{switch}i}, t, k\Big) \\ - u_B\Big(I_{B2}^{\mathrm{switch}i}, t, k\Big)\Big), \\ \forall i \in \mathrm{S_S}, \quad t \in \mathrm{S_{RT}}, \quad k \in \mathrm{S_M} \end{aligned} \tag{19}$$

$$\begin{aligned} u_S\left(i,t\right) \leq 1 - \Big(u_B\Big(I_{B2}^{\mathrm{switch}i}, t, k\Big) \\ - u_B\Big(I_{B1}^{\mathrm{switch}i}, t, k\Big)\Big), \\ \forall i \in \mathrm{S_S}, \quad t \in \mathrm{S_{RT}}, \quad k \in \mathrm{S_M} \end{aligned} \tag{20}$$

Once a switch i is closed, it cannot be opened.

$$u_S\left(i, t-1\right) \leq u_S\left(i,t\right), \quad \forall i \in S_S, \quad t \in S_{RT} \tag{21}$$

6) CRITICAL LOAD ENERGIZING CONSTRAINTS

Critical load i can be picked up once its connected bus is energized.

$$\begin{aligned} u_{CL}\left(i,t,k\right) \leq u_B\left(I_B^{\mathrm{CL}i}, t, k\right), \\ \forall i \in \mathrm{S_{CL}}, \quad t \in \mathrm{S_{RT}}, \quad k \in \mathrm{S_M} \end{aligned} \tag{22}$$

$$u_{CL}\left(i,t\right) \leq 1, \quad \forall i \in \mathrm{S_{CL}}, \quad t \in \mathrm{S_{RT}} \tag{23}$$

$$\begin{aligned} u_{CL}\left(i,t\right) \leq \sum_{k \in \mathrm{S_M}} u_{CL}\left(i,t,k\right), \\ \forall i \in \mathrm{S_{CL}}, \quad t \in \mathrm{S_{RT}} \end{aligned} \tag{24}$$

Once a critical load is picked up, it cannot be de-energized.

$$u_{CL}\left(i, t-1\right) \leq u_{CL}\left(i,t\right), \quad \forall i \in S_{CL}, \quad t \in S_{RT} \tag{25}$$

7) MICROGRID ENERGIZING CONSTRAINT

Each available microgrid is energized. It has the same energizing status with its connected bus at any time step.

8) ISLAND-WIDE REAL POWER BALANCE CONSTRAINT

One island may have multiple microgrids and it is assumed that they have sufficient power to serve the critical loads. As power loss is not considered in this model, a coefficient β is used. It requires β percentage of the total capacity of microgrids to be no less than the total real power demand of critical loads in this island.

$$\begin{aligned} \beta \cdot \sum_{k \in \mathrm{S_M}} u_M\left(i,t,k\right) \cdot P_{\mathrm{M}k} \\ \geq \sum_{j \in \mathrm{S_{CL}}} u_{CL}\left(j,t,i\right) \cdot \left(\sum_{l \in \mathrm{S_{PH}}} P_{\mathrm{CL}j}^{\mathrm{PH}l}\right), \\ \forall i \in \mathrm{S_M}, \quad t \in \mathrm{S_{RT}} \end{aligned} \tag{26}$$

F. MICROGRID NETWORK MODEL

The networked microgrids require synchronization of microgrids. For a set of n microgrids (denoted as S_{M}^{syn}) that can be synchronized, the shortest path between each pair of microgrids is searched. The length of a synchronization path is

defined as the minimum time needed to establish this path. It is defined as $T_{syn}^{MGi,j}$ and can be calculated by:

$$T_{syn}^{MGi,j} = \sum_{k \in S_L^{MGi,j}} T_L^k + \sum_{k \in S_S^{MGi,j}} T_S^k + T_{syn-scope}^{MGi,j}, \quad \forall i,j \in S_{\mathrm{M}}^{syn} \tag{27}$$

where $S_L^{MGi,j}$ and $S_S^{MGi,j}$ are the sets of all lines and switches along this path, respectively. $T_{syn-scope}^{MGi,j}$ is the time needed for operating the synchroscope at the tie switch $L_{tie-switch}^{MGi,j}$. That is, at $t = T_{syn}^{MGi,j}$, the synchronization of islands with microgrid i and j can be completed. In the real operation, however, it is possible that the synchronization may take longer. Thus, it is reasonable to optimize the restoration of these two islands independently until a timestep before $T_{syn}^{MGi,j}$ and together starting from $T_{syn}^{MGi,j}$.

A graph, $G = (N, E)$, represents a network of n microgrids. The set of nodes/microgrids and edges/paths is denoted by $N = \{1, 2, \ldots, n\}$ and $E \subseteq N \times N$, respectively. If a path between microgrid i and j is found, the weight of this edge is set as $T_{syn}^{MGi,j}$. Thus, a minimum spanning tree search [13] can be performed to select $(n-1)$ optimal paths (denoted as set $S_L^{msp} = \left\{S_L^{MGi,j}\right\}$) that interconnect these n microgrids. The lengths of synchronization paths and synchroscope operation time are denoted as $T_{msp} = \left\{T_{syn}^{MGi,j}\right\}$ and $T_{msp}^{syn-scope} = \left\{T_{syn-scope}^{MGi,j}\right\}$, respectively. The following constraints are added:

- Before microgrids i and j are synchronized, none of the buses can be affiliated with both microgrids.

$$u_B\left(m, T_{syn}^{MGi,j}-1, i\right) + u_B\left(m, T_{syn}^{MGi,j}-1, j\right) \leq 1 \quad \forall m \in \mathrm{S_B}, \quad T_{syn}^{MGi,j} \in T_{msp} \tag{28}$$

- All the lines and switches along the path that synchronizes microgrid i and j are closed at time $T_{syn}^{MGi,j}$.

$$u_L\left(m, T_{syn}^{MGi,j}\right) = u_L\left(m, T_{syn}^{MGi,j}\right) = 1 \quad \forall m \in S_L^{MGi,j}, \quad T_{syn}^{MGi,j} \in T_{msp} \tag{29}$$

$$u_S\left(m, T_{syn}^{MGi,j}\right) = u_S\left(m, T_{syn}^{MGi,j}\right) = 1 \quad \forall m \in S_S^{MGi,j}, \quad T_{syn}^{MGi,j} \in T_{msp} \tag{30}$$

- Tie switch $L_{tie-switch}^{MGi,j}$ cannot be closed before $t = T_{syn}^{MGi,j}$. Both buses of this tie switch must be energized before operating the synchroscope. That is, except for tie switch $L_{tie-switch}^{MGi,j}$, other lines and switches along the path that synchronizes microgrids i and j need to be closed no later than $t = T_{syn}^{MGi,j} - T_{syn-scope}^{MGi,j}$.

$$u_S\left(L_{tie-switch}^{MGi,j}, T_{syn}^{MGi,j}-1\right) = 0 \quad \forall T_{syn}^{MGi,j} \in T_{msp} \quad u_S\left(m, T_{syn}^{MGi,j} - T_{syn-scope}^{MGi,j}\right) = 1 \tag{31}$$

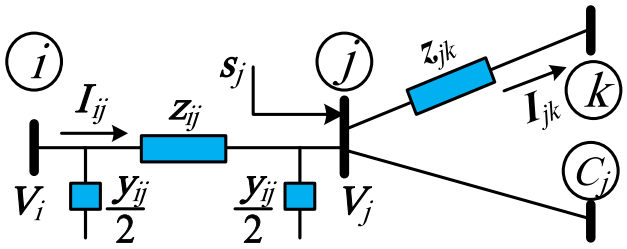

FIGURE 3. Branch power flows for a radial network.

$$u_L\left(k, T_{syn}^{MGi,j} - T_{syn-scope}^{MGi,j}\right) = 1 \quad \forall m \in \left(S_S^{MGi,j} - \left\{L_{tie-switch}^{MGi,j}\right\}\right), \quad k \in S_L^{MGi,j}, \quad T_{syn}^{MGi,j} \in T_{msp} \tag{32}$$

- Furthermore, once critical load i is picked up, it should remain the same affiliation with its connected bus.

$$u_{CL}(i,t,m) \leq 1 - \left(u_{CL}(i,t,k) - u_B\left(I_B^{CLi}, t, k\right)\right) \quad \forall i \in \mathrm{S_{CL}}, \quad t \in \mathrm{S_{RT}}, m, \quad k \in \mathrm{S_M} \tag{33}$$

$$u_{CL}(i,t,m) \leq 1 - \left(u_B\left(I_B^{CLi}, t, k\right) - u_{CL}(i,t,k)\right) \quad \forall i \in \mathrm{S_{CL}}, \quad t \in \mathrm{S_{RT}}, m, \quad k \in \mathrm{S_M} \tag{34}$$

V. MODULE-II

Module-II solves the 3Ph-OPF problem to check the voltage, current, and power constraints for the restoration actions from Module-I. The topology of the system given by the proposed restoration plan of Module-I may result in islanded areas where one or multiple resources are available to supply the critical loads. In this work, an intelligent algorithm has been developed to identify the islanded areas based on the restoration topology proposed by Module-I. Next, the algorithm formulates an individual OPF model for each islanded area. The area header node is chosen to be the largest power resource including the available microgrids, PVs, and storage devices. The sequential list of restoration actions can be evaluated one at a time, or together (simultaneously, depending upon their available resources to execute the switching actions. A major issue for system restoration is to avoid over voltage conditions due to shunt capacitances on long lines or underground cables. during early stages of the restoration procedure. Hence, minimization of the total reactive power injection due to shunt capacitances in the system is used as the objective function. Reactive power is a convex and quadratic function of bus voltages, providing conditions to its implementation as a second-order cone quadratic programing [41]. The 3Ph-OPF is implemented as a branch flow model, which is widely used for radial networks due to its numerical stability compared with the bus injection model [41]–[43].

Consider a radial distribution feeder with a set $\mathcal{N}$ of nodes $\mathcal{N} := \{0, 1, \cdots, N\}$ and a set $\mathcal{B}$ of branches $\mathcal{B} := \{1, \cdots, B\}$. A illustration of the radial structure and nodes dependency is given in Figure 3. The feasible region of the OPF model is defined by a set of linear and positive

semidefinite non-linear constraints where bus voltages, branch currents, branches flow power, and bus power injections, are related. After the *rank-1* relaxation of the 3Ph-OPF model, the secure operation region is defined by the following constraints:

$$v_j = v_i - z_{ij}S_{ij}^H - S_{ij}z_{ij}^H + z_{ij}l_{ij}z_{ij}^H, \quad \forall i \in \mathcal{N}_+ \tag{35}$$

$$s_j \geq diag\left(S_{ij} - z_{ij}l_{ij} + \frac{y_{jj}}{2}v_j - \sum_{k\in C_j} S_{jk}\right) \geq 0 \quad \forall j \in \mathcal{N}_+$$

$$\begin{pmatrix} v_i & S_{ij} \\ S_{ij}^H & l_{ij} \end{pmatrix} \succcurlyeq 0, \quad \forall i \in \mathcal{N}_+ \tag{36}$$

$$\underline{v_j} \leq v_j^{[\phi],[\phi]} \leq \overline{v}_j, \quad \forall j \in \mathcal{N}_+,\ \phi \in \Phi_j \tag{37}$$

$$s_j^\phi = p_j^\phi + \boldsymbol{j} q_j^\phi, \quad \forall j \in \mathcal{N},\ \phi \in \Phi_j \tag{38}$$

$$\underline{p_j^\phi} \leq p_j^\phi \leq \overline{p}_j^\phi, \quad \forall j \in \mathcal{N}_{CL},\ \phi \in \Phi_j \tag{39}$$

$$\underline{q_j^\phi} \leq q_j^\phi \leq \overline{q}_j^\phi, \quad \forall j \in \mathcal{N}_{CL},\ \phi \in \Phi_j \tag{40}$$

$$\left(p_j^\phi\right)^2 + \left(q_j^\phi\right)^2 \leq \left(\overline{s}_j^\phi\right)^2, \quad \forall j \in \mathcal{N}_P,\ \phi \in \Phi_j \tag{41}$$

where each node $j \in \mathcal{N}_+$ is supplied from node i, through "$i-j$" branch. Also, $\phi \in \Phi_j \subset \{a, b, c\}$ is the set of phases connected to each node j. Similarly, voltages and power injections at node j are represented by column vectors $V_j = \left[V_j^\phi\right]$, $s_j = \left[s_j^\phi\right]$, respectively. Currents flowing through each branch $(i-j) \in \mathcal{B}$ are represented by column vector $I_{ij} = \left[I_{ij}^\phi\right]$. Header node of the radial system is named as node 0, set $\mathcal{N}_+ \subset \mathcal{N}$ is defined as $\mathcal{N}_+ := \{1, \ldots, N\}$, C_k is the set of nodes directly connected downstream to node j. $\mathcal{N}_L$ represents the set of nodes where controllable load are connected, and $\mathcal{N}_P$ represents the set of nodes where power supply is available. Also, matrices $v_j \in \mathbb{C}^{|\phi|\times|\phi|}$, $l_{ij} \in \mathbb{C}^{|\phi|\times|\phi|}$, and $S_{ij} \in \mathbb{C}^{|\phi|\times|\phi|}$, where $\phi \in \Phi_j \subset \{a, b, c\}$, are calculated as $V_j V_j^H$, $I_{ij}I_{ij}^H$, $V_i I_{ij}^H$, respectively. Diagonal entries of matrix v_j are denoted as $v_j^{[\phi],[\phi]}$. Matrix $z_{ij} \in \mathbb{C}^{|\phi|\times|\phi|}$ represents the impedance between nodes $i-j$ and matrix $y_{jj} \in \mathbb{C}^{|\phi|\times|\phi|}$ is the total shunt effect given by lines connected at bus j. Kirchhoff laws are represented in (35) and (36), *rank-1* relaxed second-order cone relation between v_i, S_{ij}, and l_{ij}, is presented in (37), and other system physical requirements are represented in (38)-VI. The objective function to minimize reactive power injection due to shunt capacitances is formulated as:

$$Min \sum_{i\in\mathcal{N}_+} trace\left(imag\left(Y_i v_i\right)\right) \tag{42}$$

The provided formulation is non-linear but convex after the *rank-1* relaxation. An optimal solution of a convex problem is globally optimal [47]. Moreover, as shown in [42], [43], the relaxed 3Ph-OPF is exact, i.e. matrix in (37) results in a *rank-1* array when the system is radial. In the implementation of the OPF, branch power losses (with a sufficiently small weighting factor) are included to avoid computational issues in obtaining the exact (*rank-1*) solutions for variables v_j and l_{ij}. For non-constant power load models, a *load-update* method, as described in *Algorithm I*, has been developed in this study.

The capacitor bank injection can be modeled in the OPF problem with a relaxed integer decision variable $u_j Q_j$ in constraint (36). The relaxed decision variable is u_j ($u_j \in [0, 1]$) and the reactive power injection is Q_j (a given value). Also, a penalizing term $M\left(u_j^2 - u_j\right)$ is included in the objective function (M is a large parameter). However, this approach may not work for large scale systems, could further increase the computational burden, and may result into an inexact *rank-1* solution. Therefore, the proposed heuristic step 5, is designed to solve this problem. It can be extended to model transformer tap changers. For those cases where Module-II detects that mitigation actions are not sufficient to address the security issues, it is necessary to rebuild the restoration path (Module-I).

VI. RESULTS

IEEE 123-node test feeder [48] is used to validate the proposed restoration approach. Two cases (with and without networked microgrids) are presented for comparison. There are 10 critical loads (CLs) and 3 microgrids (MGs) as shown in Tables 1 and 2. Nine switches are assumed as the sources of uncertainty. Locations of switches are shown in Figure 4. As DSO knows the operable switches, the field crew can be sent to check the operability of the uncertain switches. In this application it is assumed that operability of all switches is known, except for Sw5 and Sw9. The information/messages from the field crew will be received by DSO on an asynchronous basis.

Module-I is modeled using AMPL (A Mathematical Programming Language) [49] and solved by Gurobi [50]. Module-II is implemented in MATLAB and solved with CVX [51]. The coordination between the modules is developed in MATLAB. A desktop with Intel Core i7-8700 (3.2 GHz processor) CPU is used in both cases.

Module-I allows to determine the optimal amount of critical load that can be restored. For "Case 1," 154 kW represented by critical loads CL1, CL3, CL5, CL6, and CL7, is restored, i.e. 73 kW, 19 kW, and 62 kW of load are restored in phases A, B, and C, respectively. In this case, given that no networked microgrids are allowed, each CL is supplied by only one MG (MG1 supplies CL5 and CL6; MG2 supplies CL7; MG3 supplies CL1 and CL3). Values of parameters a_1 and a_2 in IV-E have been defined as 1 and -1, respectively. The value of restored critical load (multiplied with its criticality factors is 382 units (includes criticality factor). Four switching actions are required. The obtained topology is shown in Figure 4. Switches Sw2, Sw3, Sw5, and Sw9 are closed. Switching actions should be performed sequentially to avoid unexpected scenarios generated by large modifications in system configuration. The remaining switches are not operated. The 3Ph-OPF evaluation in Module-II did not report any

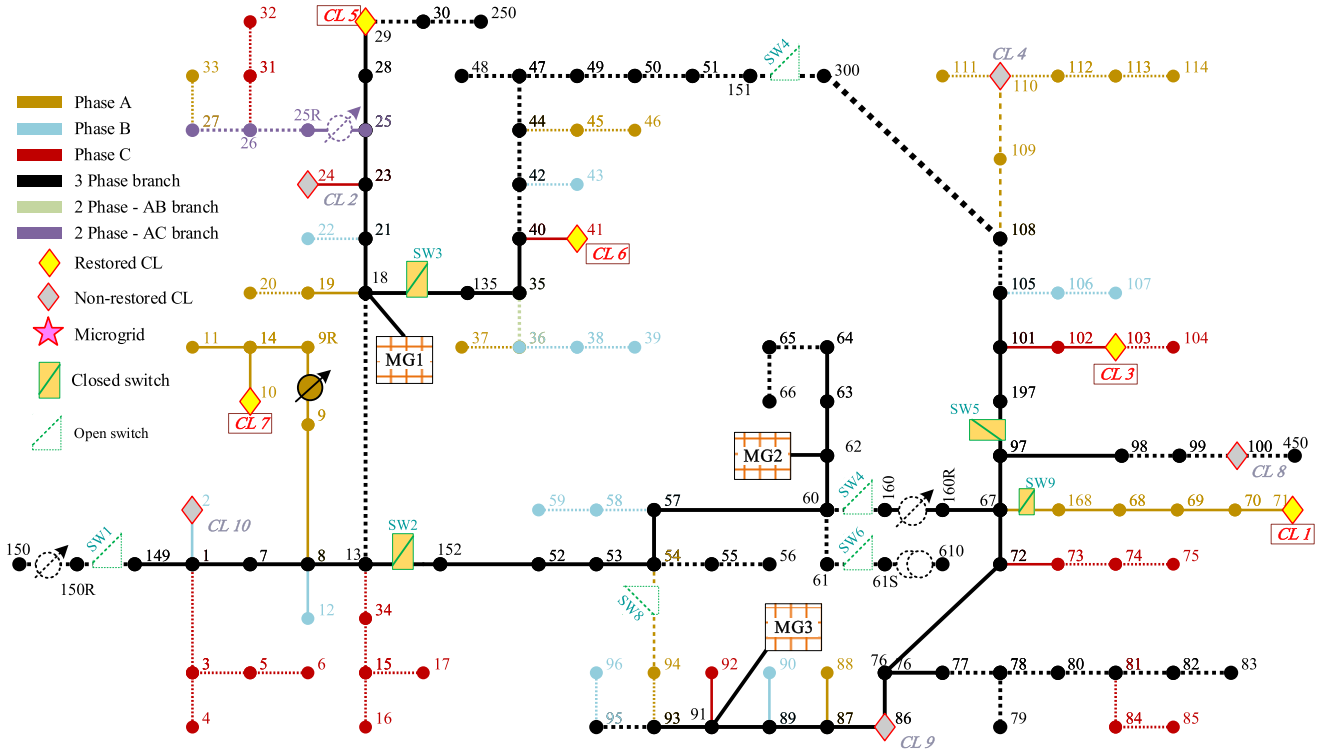

FIGURE 4. IEEE 123-node test feeder. Case 1 topology is represented as solid (energized) and dashed (non-energized) lines.

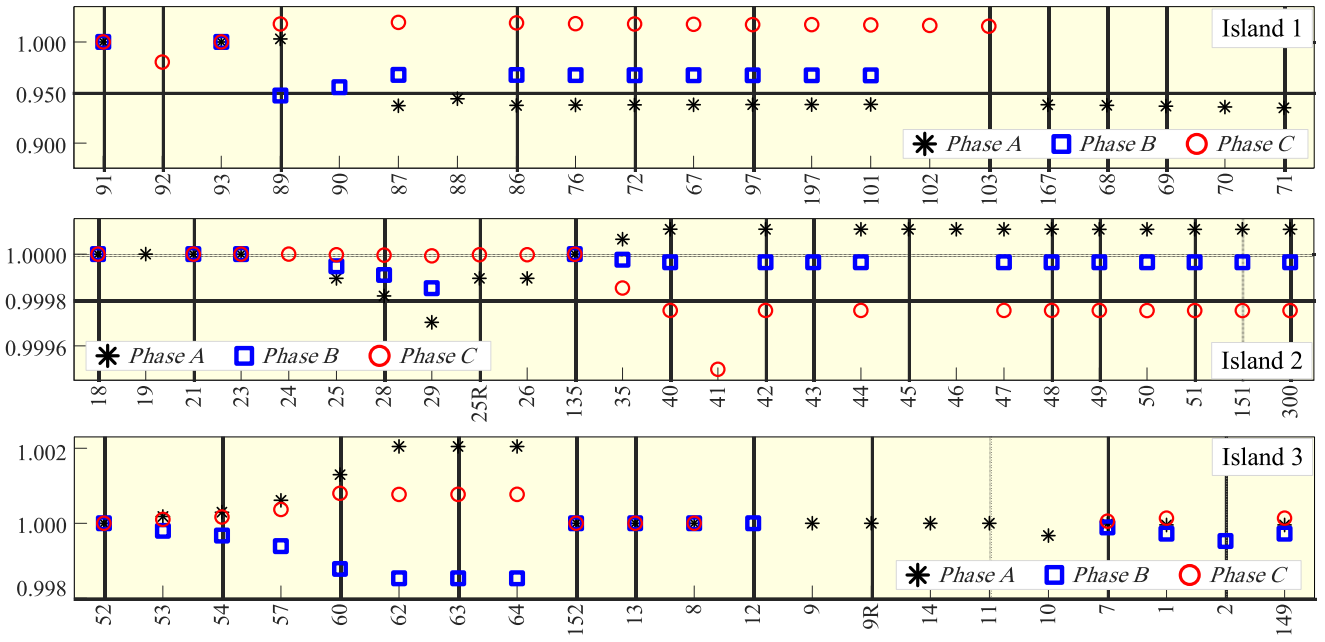

FIGURE 5. Bus voltages magnitudes (p.u.). Results of Case 1.

security constraint violation. Obtained bus voltages are presented in Figure 5. It can be seen that all of them are between the admissible range (0.90 p.u. to 1.05 p.u.). Note that the proposed objective function is to minimize shunt capacitance reactive power injections. This function depends of the line characteristics (parameters of the system) and nodal voltages.

The voltages follow a reduction pattern from the header node to the farther buses of each islanded area. However, the reduction is not considerable given that load being restored represents less than 5% of the total load of the system and some branches are operating with zero load. Note that β factor constitutes a security factor to maintain voltages

Algorithm 1 OPF Model Considering Non-Constant Power Loads

1: ***Configuration:***
- Upload system parameters: Z_{ij}, Y_{ij}, critical loads to be restored (from Module-I), and available resources to supply critical loads.
- Identify islanded areas in the restoration plan, based on largest power resources (headers) and system topology (from Module-I).
- Formulate independent OPF problems for each islanded area.
- Set bus voltages and angles as 1, $e^{j\pi/3}$, and $e^{-j\pi/3}$ p.u.
- Set k = 0 and $\boldsymbol{V}[k]$ as present nodal voltages of the system.

2: ***Update Load values***
- For non-constant power loads, update load values based on nodal voltages $\boldsymbol{V}[k]$.

3: ***Calculate the 3Ph-OPF***
- Set k = k + 1.
- Run OPFs for each island.

If feasible solution is obtained, *then*
Update decision variables v_j, s_{ij}, l_{ij}.
Update nodal voltages $\mathbf{V}[k]$
Go to step 4.
Elseif Use transformer's TAP and capacitor banks available
Go to step 5.
Else
Go to Module-I →
Search new restoration plan

4: **Convergence Evaluation**
- Evaluate differences of bus voltages $\mathbf{V}[k] - \mathbf{V}[k-1]$

If "$\mathbf{V}[k]$ vs $\mathbf{V}[k-1]$" $\notin$ "Tolerance" *then*
Go to Step 2
Else
Return nodal voltages, branch flow power, and bus power injections.

5: **Heuristic step**
- Modify tap-changer position.
- Modify reactive power injections from capacitor banks.
- Go to Step 3.

End of Algorithm 1

between the acceptable limits. The execution of Module-I takes an average of 4.3 seconds while execution of 3Ph-OPF in Module-II takes an average of 3.97 seconds.

In Case 2, networked microgrids are allowed. As a result, critical loads CL1, CL2, CL3, CL5, and CL9 are restored, i.e. 215 kW in total (89 kW in phases A, 36 kW in phases B, and 90 kW in phases C). All three microgrids are interconnected in the obtained solution. 552 units of critical load (include criticality factor) have been restored. Note the improvement in the results when the microgrid networking is allowed. Similarly, Module-II does not present any constraint violation, and obtained voltages are similar to those for case 1.

TABLE 1. Parameters of available microgrids.

	Node	Available Power, per Phase (kW)			Total Power (kW)
		A	B	C	
MG 1	18	36	36	36	108
MG 2	62	71	0	0	71
MG 3	91	48	48	48	144

TABLE 2. Parameters of Critical loads in the system.

	Node	Criticality Factor	Rated Power, per Phase (kW)			Restored Critical Loads	
			A	B	C	Case 1	Case 2
CL 1	71	2	40			Yes	Yes
CL 2	24	3			40		Yes
CL 3	103	3			37	Yes	
CL 4	110	2	36				Yes
CL 5	29	3	13	19	13	Yes	Yes
CL 6	41	3			12	Yes	
CL 7	10	1	20			Yes	
CL 8	100	1	10	20	18		
CL 9	86	2	20	6	13		Yes
CL 10	2	2		17			Yes

Finally, a discussion about the asynchronous message arrival is provided here. Consider the critical loads, CL1 and CL3, supplied by MG03 in Case 1. Note that MG03 is supplying 77 kW, represented by 40 kW, 0 kW, and 37 kW, in phases A, B, and C, respectively. The value of objective function for this restoration plan is 191 units (criticality factor included). This result was obtained in the scenario where switches Sw5 and Sw9 are available. In traditional approaches for distribution restoration, since the operability status of Sw5 and Sw9 is uncertain, the DSO can decide to restore CL8 and CL9. In that case, the restoration represents 56 kW of critical load (20 kW for phase A, 23 kW for phase B, and 13 kW for phase C), equivalents to 126 units considering criticality factors. As discussed in section II.B, equation IV, $UB = 191$, while $LB = 126$. Hence, the time that DSO should wait before compromising its decision for the non-optimal scenario is no more than 34% of the total time T^O.

$$t_w \leq \frac{(UB - LB) \cdot T^O}{UB} = \frac{191 - 126}{191} T^O = 34\% T^O \tag{43}$$

With the proposed approach, DSO has a criterion to determine how much time it should wait to receive the *asynchronous* messages from the field crew about the operability

of Sw5 and Sw9. If DSO proceeds with the restoration of CL8 and CL9, and then receives positive confirmation of Sw5 and Sw9 operability, it will not be able to reach the optimal restoration plan (restoring CL1 and CL3), resulting in an underutilization of power available from MG3.

VII. CONCLUSION

In this paper, the concept of asynchronous information is incorporated in the resiliency for distribution systems. An efficient restoration method is proposed using the two-module architecture, in which restoration plans are obtained from a BLP module and evaluated by means of an efficient 3Ph-OPF module. Impacts of the asynchronous and uncertain information are considered. In addition, it allows the interconnection of microgrids and other power resources, resulting in an enhanced usage of available generation resources. The proposed approach is also suitable to include uncertainty in the power production from renewable energy resources. Further extension of this work includes a module for checking the dynamics of switching operations and the synchronization of microgrids.

ACKNOWLEDGMENT

The authors would like to thank Dr. Sijie Chen from Shanghai Jiao Tong University for his contributions. The co-author, Dr. Xie, contributed to this project when he worked at Power and Energy Center (PEC) of Virginia Tech.

REFERENCES

[1] *IEEE Recommended Practice for the Design of Reliable Industrial and Commercial Power Systems*, IEEE Standard 493-2007, Jun. 2007, pp. 1–426.

[2] M. Panteli and P. Mancarella, "The grid: Stronger, bigger, smarter?: Presenting a conceptual framework of power system resilience," *IEEE Power Energy Mag.*, vol. 13, no. 3, pp. 58–66, May/Jun. 2015.

[3] (Feb. 12, 2013). *Presidential Policy Directive—Critical Infrastructure Security and Resilience*. [Online]. Available: https://obamawhitehouse.archives.gov/the-press-office/2013/02/12/presidential-policy-directive-critical-infrastructure-security-and-resil

[4] *National Disaster Recovery Framework*. Accessed: Feb. 23, 2019. [Online]. Available: https://www.fema.gov/national-disaster-recovery-framework

[5] L. Che, M. Khodayar, and M. Shahidehpour, "Only connect: Microgrids for distribution system restoration," *IEEE Power Energy Mag.*, vol. 12, no. 1, pp. 70–81, Jan./Feb. 2014.

[6] *RMS Estimates Insured Losses From Hurricane Florence Will Be Between USD $2.8 Billion and USD $5.0 Billion*. Accessed: Feb. 21, 2019. [Online]. Available: https://www.rms.com/newsroom/press-releases/press-detail/2018-09-24/rms-estimates-insured-losses-from-hurricane-florence-will-be-between-usd-28-billion-and-usd-50-billion

[7] *RMS Estimates Insured Losses from Hurricane Michael To Be Between USD $6.8 Billion and $10 Billion*. Accessed: Feb. 21, 2019. [Online]. Available: https://www.rms.com/newsroom/press-releases/press-detail/2018-10-19/rms-estimates-insured-losses-from-hurricane-michael-to-be-between-usd-68-billion-and-10-billion

[8] Eaton. *Responding to the Midwest Floods of 2008*. Accessed: Feb. 23, 2019. [Online]. Available: http://www.eaton.com/ecm/idcplg?IdcService=GET_FILE&dID=206651

[9] J. S. M. Coleman and D. Budikova, "Atmospheric aspects of the 2008 midwest floods: A repeat of 1993?" *Int. J. Climatol.*, vol. 30, no. 11, pp. 1645–1667, 2010.

[10] M. Mansfield and W. Linzey, "Hurricane sandy multi-state outage & restoration report," NASEP, Arlington, VA, USA, Tech. Rep. 9308, p. 23.

[11] H. Rifai, "Lessons from hurricane ike," in *Hurricane Impacts Critical Infrastructures*. Austin, TX, USA: Univ. of Texas Press, 2012, pp. 122–137.

[12] O. Hoegh-Guldberg, D. Jacob, M. Taylor, M. Bindi, S. Brown, I. Camilloni, A. Diedhiou, R. Djalante, K. L. Ebi, F. Engelbrecht, J. Guiot, Y. Hijioka, S. Mehrotra, A. Payne, S. I. Seneviratne, A. Thomas, R. Warren, and G. Zhou, "Impacts of 1.5° C global warming on natural and human systems," in *Global Warming of 1.5° C. An IPCC Special Report on the impacts of Global Warming of 1.5° C Above Pre-Industrial Levels and Related Global Greenhouse Gas Emission Pathways, in the Context of Strengthening the Global Response to the Threat of Climate Change, Sustainable Development, and Efforts to Eradicate Poverty*, V. Masson-Delmotte, P. Zhai, H.-O. Pörtner, D. Roberts, J. Skea, P. R. Shukla, A. Pirani, W. Moufouma-Okia, C. Péan, R. Pidcock, S. Connors, J. B. R. Matthews, Y. Chen, X. Zhou, M. I. Gomis, E. Lonnoy, T. Maycock, M. Tignor, and T. Waterfield, Eds. 2018.

[13] M. Held and R. M. Karp, "The traveling-salesman problem and minimum spanning trees: Part II," *Math. Program.*, vol. 1, no. 1, pp. 6–25, Dec. 1971.

[14] T. S. Lee, S. Ghosh, and A. Nerode, "A mathematical framework for asynchronous, distributed, decision-making systems with semi-autonomous entities: Algorithm synthesis, simulation, and evaluation," in *Proc. 4th Int. Symp. Auton. Decentralized Syst.*, Mar. 1999, pp. 206–212. [Online]. Available: https://ieeexplore.ieee.org/document/838435.

[15] S. Choi, "Practical coordination between day-ahead and real-time optimization for economic and stable operation of distribution systems," *IEEE Trans. Power Syst.*, vol. 33, no. 4, pp. 4475–4487, Jul. 2018.

[16] L. Wang, A. J. Vega, A. Buyuktosunoglu, P. Bose, and K. Skadron, "Power-efficient embedded processing with resilience and real-time constraints," in *Proc. IEEE/ACM Int. Symp. Low Power Electron. Design (ISLPED)*, Jul. 2015, pp. 231–236.

[17] T.-F. Li and H. Wang, "Asynchronous switching control for switched delay systems induced by sampling mechanism," *IEEE Access*, vol. 6, pp. 10787–10794, 2018.

[18] N. T. Raknes, K. Ødeskaug, M. Stålhane, and L. M. Hvattum, "Scheduling of maintenance tasks and routing of a joint vessel fleet for multiple offshore wind farms," *J. Mar. Sci. Eng.*, vol. 5, no. 1, p. 11, Mar. 2017.

[19] J. M. Solanki, S. Khushalani, and N. N. Schulz, "A multi-agent solution to distribution systems restoration," *IEEE Trans. Power Syst.*, vol. 22, no. 3, pp. 1026–1034, Aug. 2007.

[20] C.-C. Liu, S. J. Lee, and S. S. Venkata, "An expert system operational aid for restoration and loss reduction of distribution systems," *IEEE Trans. Power Syst.*, vol. 3, no. 2, pp. 619–626, May 1988.

[21] A. L. Morelato and A. Monticelli, "Heuristic search approach to distribution system restoration," *IEEE Trans. Power Del.*, vol. 4, no. 4, pp. 2235–2241, Oct. 1989.

[22] S. I. Lim, S. J. Lee, M. S. Choi, D. J. Lim, and B. N. Ha, "Service restoration methodology for multiple fault case in distribution systems," *IEEE Trans. Power Syst.*, vol. 21, no. 4, pp. 1638–1644, Nov. 2006.

[23] R. E. Perez-Guerrero and G. T. Heydt, "Distribution system restoration via subgradient-based lagrangian relaxation," *IEEE Trans. Power Syst.*, vol. 23, no. 3, pp. 1162–1169, Aug. 2008.

[24] Y. Jiang, C.-C. Liu, M. Diedesch, E. Lee, and A. K. Srivastava, "Outage management of distribution systems incorporating information from smart meters," *IEEE Trans. Power Syst.*, vol. 31, no. 5, pp. 4144–4154, Sep. 2016.

[25] Y. Xu, C.-C. Liu, K. P. Schneider, and D. T. Ton, "Placement of remote-controlled switches to enhance distribution system restoration capability," *IEEE Trans. Power Syst.*, vol. 31, no. 2, pp. 1139–1150, Mar. 2016.

[26] B. Wang, Y. Wang, H. Nazaripouya, C. Qiu, C.-C. Chu, and R. Gadh, "Predictive scheduling framework for electric vehicles with uncertainties of user behaviors," *IEEE Internet Things J.*, vol. 4, no. 1, pp. 52–63, Feb. 2017.

[27] Y. Wang, B. Wang, C.-C. Chu, H. Pota, and R. Gadh, "Energy management for a commercial building microgrid with stationary and mobile battery storage," *Energy Buildings*, vol. 116, pp. 141–150, Mar. 2016.

[28] C. Chen, J. Wang, F. Qiu, and D. Zhao, "Resilient distribution system by microgrids formation after natural disasters," *IEEE Trans. Smart Grid*, vol. 7, no. 2, pp. 958–966, Mar. 2016.

[29] Argonne National Laboratory. *A Three-Phase Microgrid Restoration Model Considering Unbalanced Operation of Distributed Generation*. Accessed: Feb. 25, 2019. [Online]. Available: https://argonne-scientific-publications/pub/131260

[30] S. Khushalani, J. M. Solanki, and N. N. Schulz, "Optimized restoration of unbalanced distribution systems," *IEEE Trans. Power Syst.*, vol. 22, no. 2, pp. 624–630, May 2007.

[31] B. Chen, C. Chen, J. Wang, and K. L. Butler-Purry, "Sequential service restoration for unbalanced distribution systems and microgrids," *IEEE Trans. Power Syst.*, vol. 33, no. 2, pp. 1507–1520, Mar. 2018.

[32] J. Li, X.-Y. Ma, C.-C. Liu, and K. P. Schneider, "Distribution system restoration with microgrids using spanning tree search," *IEEE Trans. Power Syst.*, vol. 29, no. 6, pp. 3021–3029, Nov. 2014.
[33] A. Sharma, D. Srinivasan, and A. Trivedi, "A decentralized multiagent system approach for service restoration using DG islanding," *IEEE Trans. Smart Grid*, vol. 6, no. 6, pp. 2784–2793, Nov. 2015.
[34] Y. Ren, D. Fan, Q. Feng, Z. Wang, B. Sun, and D. Yang, "Agent-based restoration approach for reliability with load balancing on smart grids," *Appl. Energy*, vol. 249, pp. 46–57, Sep. 2019.
[35] K. P. Schneider, S. Laval, J. Hansen, R. B. Melton, L. Ponder, L. Fox, J. Hart, J. Hambrick, M. Buckner, M. Baggu, and K. Prabakar, "A Distributed Power System Control Architecture for Improved Distribution System Resiliency," *IEEE Access*, vol. 7, pp. 9957–9970, 2019.
[36] Y. Xu, C.-C. Liu, K. P. Schneider, F. K. Tuffner, and D. T. Ton, "Microgrids for service restoration to critical load in a resilient distribution system," *IEEE Trans. Smart Grid*, vol. 9, no. 1, pp. 426–437, Jan. 2018.
[37] Y. Xu, C.-C. Liu, Z. Wang, K. Mo, K. P. Schneider, F. K. Tuffner, and D. T. Ton, "DGs for service restoration to critical loads in a secondary network," *IEEE Trans. Smart Grid*, vol. 10, no. 1, pp. 435–447, Jan. 2019.
[38] K. P. Schneider, F. K. Tuffner, M. A. Elizondo, C.-C. Liu, Y. Xu, S. Backhaus, and D. T. Ton, "Enabling resiliency operations across multiple microgrids with grid friendly appliance controllers," *IEEE Trans. Smart Grid*, vol. 9, no. 5, pp. 4755–4764, Sep. 2018.
[39] K. P. Schneider, N. Radhakrishnan, Y. Tang, F. K. Tuffner, C.-C. Liu, J. Xie, and D. Ton, "Improving primary frequency response to support networked microgrid operations," *IEEE Trans. Power Syst.*, vol. 34, no. 1, pp. 659–667, Jan. 2019.
[40] A. Sharma, A. Trivedi, and D. Srinivasan, "Multi-stage restoration strategy for service restoration in distribution systems considering outage duration uncertainty," *IET Gener., Transmiss. Distrib.*, vol. 12, no. 19, pp. 4319–4326, Oct. 2018.
[41] S. H. Low, "Convex relaxation of optimal power flow—Part I: Formulations and equivalence," *IEEE Trans. Control Netw. Syst.*, vol. 1, no. 1, pp. 15–27, Mar. 2014.
[42] S. H. Low, "Convex relaxation of optimal power flow—Part II: Exactness," *IEEE Trans. Control Netw. Syst.*, vol. 1, no. 2, pp. 177–189, Jun. 2014.
[43] L. Gan and S. H. Low, "Convex relaxations and linear approximation for optimal power flow in multiphase radial networks," in *Proc. Power Syst. Comput. Conf.*, Aug. 2014, pp. 1–9.
[44] B. Cai, M. Xie, Y. Liu, Y. Liu, and Q. Feng, "Availability-based engineering resilience metric and its corresponding evaluation methodology," *Rel. Eng. Syst. Saf.*, vol. 172, pp. 216–224, Apr. 2018.
[45] Q. Feng, X. Zhao, D. Fan, B. Cai, Y. Liu, and Y. Ren, "Resilience design method based on meta-structure: A case study of offshore wind farm," *Rel. Eng. Syst. Saf.*, vol. 186, pp. 232–244, Jun. 2019.
[46] H. Gao, Y. Chen, Y. Xu, and C.-C. Liu, "Resilience-oriented critical load restoration using microgrids in distribution systems," *IEEE Trans. Smart Grid*, vol. 7, no. 6, pp. 2837–2848, Nov. 2016.
[47] S. Boyd and L. Vandenberghe, *Convex Optimization*. Cambridge, U.K.: Cambridge Univ. Press, 2004.
[48] *Distribution Test Feeders—Distribution Test Feeder Working Group—IEEE PES Distribution System Analysis Subcommittee*. Accessed: Jun. 19, 2017. [Online]. Available: https://ewh.ieee.org/soc/pes/dsacom/testfeeders/
[49] *AMPL for Research—AMPLAMPL*. Accessed: Jun. 8, 2018. [Online]. Available: https://ampl.com/products/ampl/ampl-for-research/
[50] *Gurobi Optimization—The State-of-the-Art Mathematical Programming Solver*. Accessed: Jun. 8, 2018. [Online]. Available: http://www.gurobi.com/
[51] CVX Research. *CVX: MATLAB Software for Disciplined Convex Programming*. Accessed: Jun. 19, 2017. [Online]. Available: http://cvxr.com/cvx/

JUAN C. BEDOYA received the B.S. and M.S. degrees in electrical engineering from the Technological University of Pereira, Colombia, in 2005 and 2010, respectively. He is currently pursuing the Ph.D. degree in electrical engineering with Virginia Polytechnic Institute and State University, Blacksburg, VA. From 2008 to 2016, he was a Coordinator of the wholesale electricity market transactions for the Colombian Independent System Operator and Market Administrator, XM S.A. E.S.P. His research interests include demand response, transactive energy, power systems restoration, electricity markets, and optimization for power systems. In 2016, he was honored as a Fulbright grantee.

JING XIE received the B.E. and M.S. degrees from Tongji University, China, in 2010 and 2011, respectively, and the Ph.D. degree from University College Dublin, Dublin, Ireland, in 2015. From 2016 to 2018, he was an Assistant Research Professor with the School of Electrical Engineering and Computer Science, Washington State University, Pullman, WA, USA. From 2018 to 2019, he was a Postdoctoral Associate with the Power and Energy Center, Virginia Tech. He is currently a Postdoctoral Associate with Pacific Northwest National Laboratory (PNNL). His research interests include physical security of substations, distributed control of power systems, distribution system operation, and cyber-physical system test bed technologies.

YUBO WANG received the B.S. degree in electrical engineering from Southeast University, Nanjing, China, in 2011, and the M.S. degree in electrical engineering and the Ph.D. degree in mechanical engineering from the University of California, Los Angeles, USA, in 2012 and 2017, respectively. He is currently a Research Scientist with Siemens Corporate Technology. His research interests include stochastic modeling, decentralized optimizations and data analytics with applications in power systems, and the Internet of Things.

XI ZHANG received the M.Eng. degree in electrical engineering from Imperial College London, U.K., and the Ph.D. degree in electrical engineering from RWTH Aachen University, Germany. She is currently the Head of the Embedded Web Technologies research group in the area of Internet of Things, Siemens Corporate Technology, Princeton, NJ. She is an expert in communication technologies for Industrial Internet of Things. She has a focus on the e-Mobility space in terms of standardizing the communication interface for efficient and interoperable Electric Vehicle to Grid Integration. She is currently active in ISO TC 22 and IEC TC 69.

CHEN-CHING LIU (F'94) received the Ph.D. degree from the University of California, Berkeley, CA. He is currently an American Electric Power Professor and the Director of the Power and Energy Center, Virginia Polytechnic Institute and State University, Blacksburg, VA. He is also a Research Professor with Washington State University, Pullman, WA, and a Visiting Professor with University College Dublin, Dublin, Ireland. He was a recipient of the IEEE PES Outstanding Power Engineering Educator Award and the Doctor Honoris Causa from the Polytechnic University of Bucharest, Bucharest, Romania. He was the Chair of IEEE PES Technical Committee on Power System Analysis, Computing, and Economics.